




Article

# Active Color Control in a Metasurface by Polarization Rotation

Minkyung Kim <sup>1,†</sup> , Inki Kim <sup>1,†</sup>, Jaehyuck Jang <sup>2,†</sup>, Dasol Lee <sup>1</sup> , Ki Tae Nam <sup>3</sup> and Junsuk Rho <sup>1,2,4,\*</sup> 

<sup>1</sup> Department of Mechanical Engineering, Pohang University of Science and Technology (POSTECH), Pohang 37673, Korea; kmk961120@postech.ac.kr (M.K.); inki93@postech.ac.kr (I.K.); dasol2@postech.ac.kr (D.L.)

<sup>2</sup> Department of Chemical Engineering, Pohang University of Science and Technology (POSTECH), Pohang 37673, Korea; jayjang@postech.ac.kr

<sup>3</sup> Department of Materials Science and Engineering, Seoul National University, Seoul 08826, Korea; nkitae@snu.ac.kr

<sup>4</sup> National Institute of Nanomaterials Technology (NINT), Pohang 37673, Korea

\* Correspondence: jsrho@postech.ac.kr

† These authors contributed equally to this work.

Received: 17 May 2018; Accepted: 13 June 2018; Published: 15 June 2018



**Abstract:** Generating colors by employing metallic nanostructures has attracted intensive scientific attention recently, because one can easily realize higher spatial resolution and highly robust colors compared to conventional pigment. However, since the scattering spectra and thereby the resultant colors are determined by the nanostructure geometries, only one fixed color can be produced by one design and a whole new sample is required to generate a different color. In this paper, we demonstrate active metasurface, which shows a range of colors dependent on incident polarization by selectively exciting three different plasmonic nanorods. The metasurface, which does not include any tunable materials or external stimuli, will be beneficial in real-life applications especially in the display applications.

**Keywords:** structural color printing; metasurface; active metamaterials; polarization control

## 1. Introduction

Structural color generation has received intensive research attention to color filter and display technologies for replacing conventional dye and pigment based system. Many of the structural colors, especially structural colors by metasurface, composed of periodic array of nanostructured materials, have been focused due to their compactness, near-permanent lifetime, and capability for surpassing diffraction limit to ultra-high dpi far beyond the resolution of any color-generation system. As its geometric dimensions are comparable to the wavelength of visible light, a periodic array of nanostructures exhibits optical resonances at visible wavelength, thereby producing color that corresponds to the scattering spectrum. The structural color generation by the metasurfaces has been successfully demonstrated in plasmonics [1–6] and dielectric systems [7–11] using a variety of designs (See review papers [12–16] for details). However, as the geometry of nanostructures specifies scattering properties, an array of nanostructures usually produces only one fixed color. It implies that a whole new sample should be fabricated to produce different color or temporally varying color. As an alternative, adoption of mechanical transformation [17–21], chemical transition [22–24], phase change material [25–28] and electrochromic polymer [29] provide dynamic color printing. Nevertheless, dynamic color printing can be realized in a far simpler system by polarization control without involving any external stimuli [30–32]. A periodic array of cross-shaped nanoantennas [8,33–35], elliptical nanostructures

[31,32,36], rectangle nanostructures [37] and a grating pattern [38] have demonstrated active color printing by rotating incident polarization. Here, lack of four-fold symmetry leads to active color generation. However, previously demonstrated structures cannot support wide range of colors as they generate linearly varying color gamut [33] or cover partial space [8,38] in a chromaticity diagram using one unit design. Meanwhile, generation of three primary colors: red, green and blue in a single system, has been reported by adopting three cavities of different shapes and directions altogether [30]. Although this cavity-aperture system had potential for a tunable color filter, transmittance of the system is extremely low, obstructing practical usage.

In this paper, we present and demonstrate the reflection type metasurface, producing different color under incident polarization. Whereas previous works have utilized a single anisotropic structure in a unit cell, we introduce three different nanorods which work as dipoles in order to selectively excite the nanostructures depending on incident polarization direction. As a result, we can realize circular color-changing path in color gamut providing much larger tunability. We experimentally demonstrate reflection type active color generation, which agrees well with the simulated color. Finally, we suggest the complementary design metasurface, which has three different slits on a metal film, as a transmission type metasurface based on the Babinet's principle. These metasurfaces covering a wide range of colors in a single design present a possibility of tunable color printing without complex system, which can be beneficial in real-world applications such as display and sensing.

## 2. Results

The metasurface is composed of three aluminum nanorods on a silica film, and an aluminum film of thickness 90 nm is sandwiched between the silica film and substrate. The metal-insulator-metal structure enhances the overall reflection. Three nanorods are periodically arranged, and  $i$ -th rod is tilted by  $\phi_i$  where  $a_i$  and  $b_i$  denote horizontal and vertical dimension. Detailed geometric dimensions can be found in Figure 1. When the metasurface is illuminated by visible light source, localized surface plasmon resonances formed near the nanorods offer structured reflection spectrum with multiple dips. When the rods have a rectangle shape, the metasurface optically responds differently under incident polarization due to the anisotropic geometry. Especially if the rectangle has a high aspect ratio, it can be approximated as a dipole which interacts strongly with light polarized parallel to the oscillating direction. As the optical resonances can be shifted by changing geometric dimensions and the pitch of the rod, it is possible to design three different nanorods with different resonance wavelengths and selectively excite them by matching incident polarization to the dipole moment direction.

However, since three dipoles cannot be mutually orthogonal in a plane, cross-talks between rods are unavoidable. Although  $60^\circ$  of relative direction between each rod minimizes the cross-talk, the direction of the rods also determines the periodic arrangement and hence the reflection spectrum. Therefore, directions of rods are set for desired resonance wavelength and the final dimensions of three rods are tuned through parametric sweep. The metasurface is then fabricated by electron-beam lithography and lift-off process. (See Materials and Methods section for details). A scanning electron microscopy (SEM) image of the sample is presented in Figure 1c.

Polarization sensitive reflection spectrum and the corresponding colors are presented in Figure 2. We used the Lumerical finite-difference time-domain (FDTD) solution for numerical simulation. The simulated reflection spectrum indicates that the metasurface has multiple peaks and dips over the visible range, especially 450 nm, 540 nm and 620 nm. At those resonance wavelengths, incident light may or may not excite the nanorods, and the spectra show notable distinction dependent on the polarization direction. Three distinctive nanoantennas provide active color generation sensitive to the incident polarization. As the polarization rotates from  $0^\circ$  to  $180^\circ$ , the color gamut represented in CIE 1931 space forms an oval. Although the metasurface does not produce vivid primary colors, it covers a wide range of colors in a single design. Colors generated by the fabricated sample are measured by a CCD camera implemented in a hyperion 1000 microscope (bottom panel in Figure 2c).

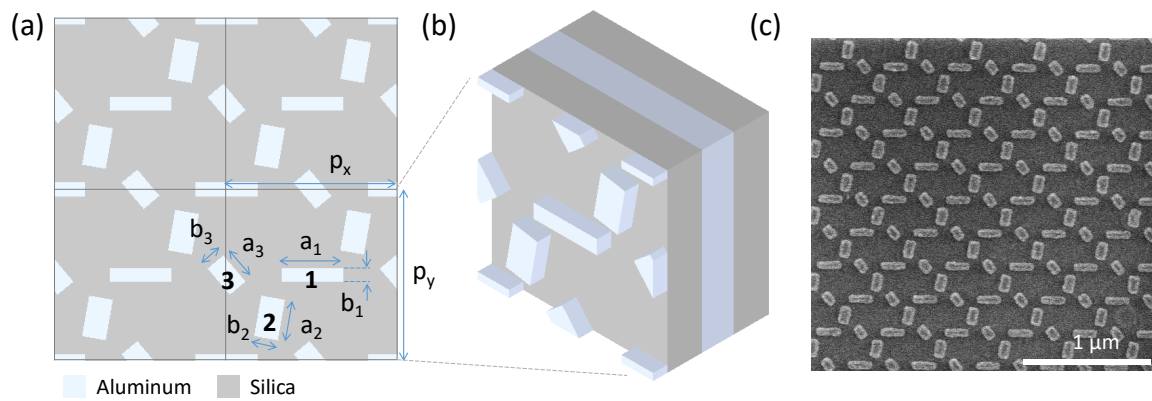


**Figure 1.** (a) Schematic of metasurface and (b) its unit cell. It has metal-insulator-metal structure where aluminum and silica are used as metal and insulator respectively on a silica substrate. Thickness of aluminum film, silica film and aluminum rods are 90 nm, 100 nm and 40 nm respectively. Three nanorods numbered by 1, 2 and 3 are periodically arranged and the unit cell has two of each of the nanorods.  $i$ -th slit is tilted by  $\phi_i$  where  $a_i$  and  $b_i$  denote horizontal and vertical dimension. Geometric parameters indicated in the figure are:  $p_x = 500$  nm,  $p_y = 500$  nm,  $a_1 = 180$  nm,  $a_2 = 120$  nm,  $a_3 = 100$  nm,  $b_1 = 40$  nm,  $b_2 = 70$  nm,  $b_3 = 60$  nm,  $\phi_1 = 0^\circ$ ,  $\phi_2 = 80^\circ$ ,  $\phi_3 = 130^\circ$ . (c) Top view of scanning electron microscopy image.

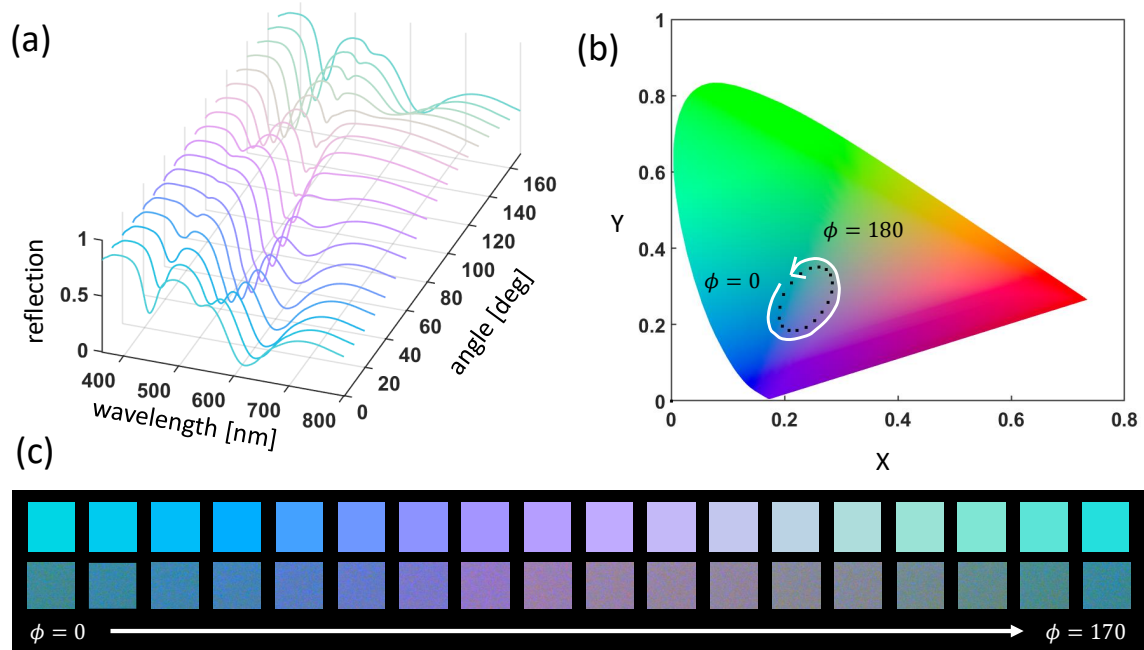


**Figure 2.** (a) Polarization dependent reflection spectrum, (b) CIE 1931 chromaticity diagram and (c) color palette. Simulated and experimentally obtained colors are shown in the first and second rows respectively. Polarization angle of incidence is represented in degree.

### 3. Discussion

Light-matter interaction at the nanostructures is further examined at three wavelengths: 450 nm, 540 nm and 620 nm where the spectra strongly depend on the incident polarization. Electric field amplitude distribution at the middle of the rods is shown in Figure 3. The incident electric field disturbs electrons' density in the vicinity of aluminum rods. Because of the anisotropic geometry of the rods, generation of this localized surface plasmons depends on both wavelength and polarization. Each rod takes charge of one resonance and forms a dip in the reflection spectrum when the incident polarization is parallel to its dipole direction. In other words, only certain polarization induces localized surface plasmon strongly in a given wavelength despite the cross-talks between nanorods. Since field oscillation leads to high absorption, the resultant reflection has a dip and generates a complementary color.

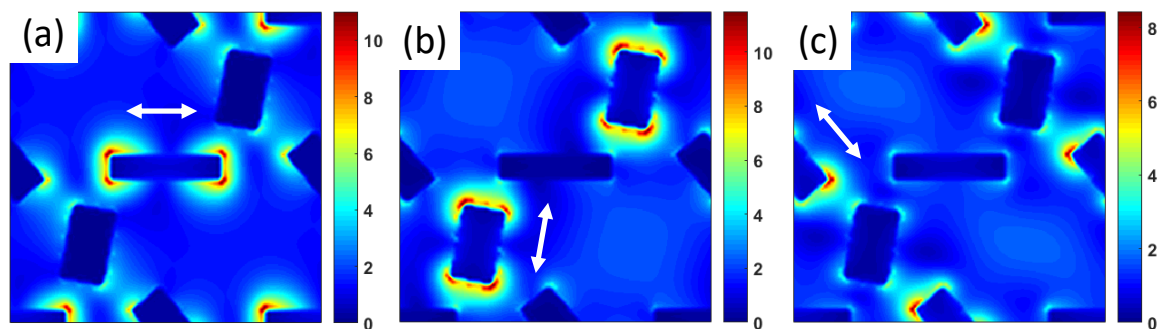


**Figure 3.** Calculated electric field distribution at the middle of the rods at (a) 620 nm, (b) 540 nm and (c) 450 nm. White arrows denote polarization angle of incidence.

According to the Babinet's principle [39,40], the reflection pattern of nanorods is identical to the transmission pattern of nanoslits. Subwavelength-perforated metal film offers a structured transmission spectrum with multiple peaks and dips, which is also known as extraordinary optical transmission [41]. Therefore, using the concept of Babinet's principle, we can also design transmission type metasurface composed of three nanoslits on aluminum film as illustrated in Figure 4a,b. Transmission type metasurface follows the same story as the reflection type. Three different nanoslits with different resonance wavelength can be selectively excited by matching incident polarization to the dipole moment direction. Figure 4c–e show the polarization dependent transmission spectra and the corresponding colors. Simulated color shows tunability of transmission type color printed upon polarization of incidence. Note that the transmission efficiency is low whereas the reflection type metasurface shows high reflection spectra originating from metal-insulator-metal structure.

In conclusion, an active metasurface which produces colors dependent on incident polarization is presented. The reflection type metasurface possessing three different nanorods responds sensitively under rotating incident polarization. We numerically and experimentally demonstrate that the reflection type metasurface covers a wide range of colors by a single design. Furthermore, we present the complementary design of metasurface for transmission type. These two types of active metasurfaces show potential to be integrated with conventional liquid crystal technology thanks to its polarization dependent optical responses. With the compatibility with electrically-driving technologies, this active color generating metasurface may be a promising candidate for future generation display with ultra-high resolution and long-lasting lifetime.

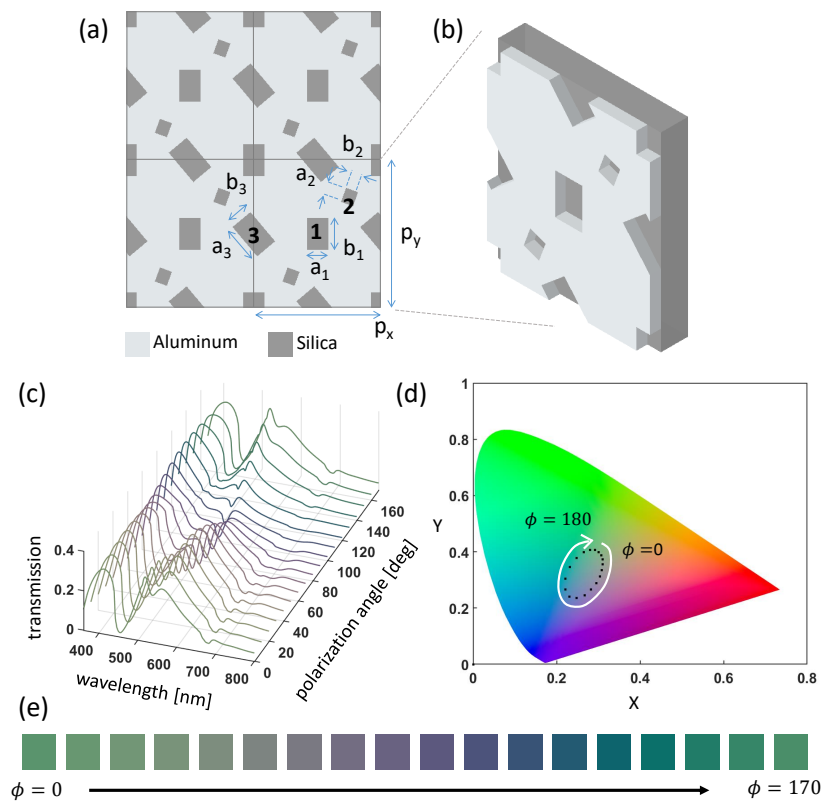


**Figure 4.** (a) Schematic of transmission type metasurface and (b) its unit cell. Aluminum film of thickness 40 nm on a silica substrate has three slits numbered by 1, 2 and 3, and the unit cell has two of each slit.  $i$ -th slit is tilted by  $\phi_i$  where  $a_i$  and  $b_i$  denote horizontal and vertical dimension. Geometric parameters indicated in the figure are:  $p_x = 600$  nm,  $p_y = 700$  nm,  $a_1 = 100$  nm,  $a_2 = 70$  nm,  $a_3 = 180$  nm,  $b_1 = 150$  nm,  $b_2 = 60$  nm,  $b_3 = 110$  nm,  $\phi_1 = 0^\circ$ ,  $\phi_2 = 70^\circ$ ,  $\phi_3 = 130^\circ$ . (c) Polarization dependent transmission spectrum. (d) CIE 1931 chromaticity diagram and (e) color palette of transmission type metasurface.

#### 4. Materials and Methods

The reflection type of active metasurface is fabricated on silicon substrate. Firstly, 90 nm thick aluminum thin film and 100 nm thick silicon dioxide layer are deposited by electron beam evaporation (Korea Vacuum Tech, Gimpo-si, Korea, KVE-ENS4004). Then, the polymethyl methacrylate (PMMA) layer is spin-coated onto the substrate. Similarly, a conductive polymer layer (Showa Denko, Tokyo, Japan, E-spacer 300Z) is also spin-coated to prevent the charging effect from the silica layer. Electron beam lithography (ELIONIX, Tokyo, Japan, ELS-7800, 80 kV, 50 pA) is used to expose nanorod patterns on photoresist. After exposing, the conductive layer is firstly removed by DI water and exposed nanorod patterns are developed by the MIBK:IPA 1:3 solutions. Finally, an adhesion layer of 3 nm thick chromium and a structure layer of 40 nm thick aluminum are deposited by electron beam evaporation and nanorod patterns are transferred onto the substrate. Then white-balanced images are collected using a  $\times 4$ , 0.07 numerical aperture objective on an optical microscope (Hyperion 1000) with LED light source (Opto Semiconductors, Regensburg, Germany, LE UW S2W) and Infinity 1-2 CCD camera.

**Author Contributions:** Conceptualization & Supervision, J.R.; Numerical simulation & Writing manuscript, M.K.; Fabrication, I.K.; Measurement, J.J. and D.L.

**Funding:** This research was funded by the LGD-SNU incubation program from LG Display and the National Research Foundation of Korea (NRF-2017R1E1A1A03070501, NRF-2015R1A5A1037668, CAMM-2014M3A6B3063708) funded by the Ministry of Science and ICT (MSIT), and Global PhD Fellowships from Korean government (NRF-2017H1A2A1043204, NRF-2016H1A2A1906519).

**Acknowledgments:** J.R. acknowledges Shuang Zhang at the University of Birmingham for the useful discussion.

**Conflicts of Interest:** The authors declare no conflict of interest.

## References

1. Wang, W.; Rosenmann, D.; Czaplewski, D.A.; Yang, X.; Gao, J. Realizing structural color generation with aluminum plasmonic V-groove metasurfaces. *Opt. Express* **2017**, *25*, 20454–20465. [[CrossRef](#)] [[PubMed](#)]
2. Cheng, F.; Gao, J.; Stan, L.; Rosenmann, D.; Czaplewski, D.; Yang, X. Aluminum plasmonic metamaterials for structural color printing. *Opt. Express* **2015**, *23*, 14552–14560. doi:10.1364/OE.23.014552. [[CrossRef](#)] [[PubMed](#)]
3. Miyata, M.; Hatada, H.; Takahara, J. Full-Color Subwavelength Printing with Gap-Plasmonic Optical Antennas. *Nano Lett.* **2016**, *16*, 3166–3172. doi:10.1021/acs.nanolett.6b00500. [[CrossRef](#)] [[PubMed](#)]
4. Olson, J.; Manjavacas, A.; Basu, T.; Huang, D.; Schlather, A.E.; Zheng, B.; Halas, N.J.; Nordlander, P.; Link, S. High Chromaticity Aluminum Plasmonic Pixels for Active Liquid Crystal Displays. *ACS Nano* **2016**, *10*, 1108–1117. doi:10.1021/acs.nano.5b06415. [[CrossRef](#)] [[PubMed](#)]
5. Kumar, K.; Duan, H.; Hegde, R.S.; Koh, S.C.W.; Wei, J.N.; Yang, J.K.W. Printing colour at the optical diffraction limit. *Nat. Nanotechnol.* **2012**, *7*, 557–561. doi:10.1038/nnano.2012.128. [[CrossRef](#)] [[PubMed](#)]
6. Lee, H.E.; Ahn, H.Y.; Mun, J.; Young Lee, Y.; Kim, M.; Heon Cho, N.; Chang, K.; Sung Kim, W.; Rho, J.; Nam, K.T. Amino-acid- and peptide-directed synthesis of chiral plasmonic gold nanoparticles. *Nature* **2018**, *556*, 360–365. [[CrossRef](#)] [[PubMed](#)]
7. Horie, Y.; Han, S.; Lee, J.Y.; Kim, J.; Kim, Y.; Arbabi, A.; Shin, C.; Shi, L.; Arbabi, E.; Kamali, S.M.; et al. Visible Wavelength Color Filters Using Dielectric Subwavelength Gratings for Backside-Illuminated CMOS Image Sensor Technologies. *Nano Lett.* **2017**, *17*, 3159–3164. doi:10.1021/acs.nanolett.7b00636. [[CrossRef](#)] [[PubMed](#)]
8. Vashistha, V.; Vaidya, G.; Gruszecki, P.; Serebryannikov, A.E.; Krawczyk, M. Polarization tunable all-dielectric color filters based on cross-shaped Si nanoantennas. *Sci. Rep.* **2017**, *7*, 8092. doi:10.1038/s41598-017-07986-z. [[CrossRef](#)] [[PubMed](#)]
9. Proust, J.; Bedu, F.; Gallas, B.; Ozerov, I.; Bonod, N. All-Dielectric Colored Metasurfaces with Silicon Mie Resonators. *ACS Nano* **2016**, *10*, 7761–7767. doi:10.1021/acs.nano.6b03207. [[CrossRef](#)] [[PubMed](#)]
10. Yoon, G.; Lee, D.; Nam, K.T.; Rho, J. Pragmatic Metasurface Hologram at Visible Wavelength: The Balance between Diffraction Efficiency and Fabrication Compatibility. *ACS Photonics* **2018**, *5*, 1643–1647. doi:10.1021/acsphotonics.7b01044. [[CrossRef](#)]
11. Li, Z.; Kim, I.; Zhang, L.; Mehmood, M.Q.; Anwar, M.S.; Saleem, M.; Lee, D.; Nam, K.T.; Zhang, S.; Luk'yanchuk, B.; et al. Dielectric Meta-Holograms Enabled with Dual Magnetic Resonances in Visible Light. *ACS Nano* **2017**, *11*, 9382–9389. doi:10.1021/acs.nano.7b04868. [[CrossRef](#)] [[PubMed](#)]
12. Lee, T.; Jang, J.; Jeong, H.; Rho, J. Plasmonic- and dielectric-based structural coloring: From fundamentals to practical applications. *Nano Converg.* **2018**, *5*, 1. doi:10.1186/s40580-017-0133-y. [[CrossRef](#)] [[PubMed](#)]
13. Kristensen, A.; Yang, J.K.W.; Bozhevolnyi, S.I.; Link, S.; Nordlander, P.; Halas, N.J.; Mortensen, N.A. Plasmonic colour generation. *Nat. Rev. Mater.* **2016**, *2*, 16088. [[CrossRef](#)]
14. Keshavarz Hedayati, M.; Elbahri, M. Review of Metasurface Plasmonic Structural Color. *Plasmonics* **2017**, *12*, 1463–1479. doi:10.1007/s11468-016-0407-y. [[CrossRef](#)]
15. Zhao, Y.; Zhao, Y.; Hu, S.; Lv, J.; Ying, Y.; Gervinskas, G.; Si, G. Artificial Structural Color Pixels: A Review. *Materials* **2017**, *10*, 944. doi:10.3390/ma10080944. [[CrossRef](#)] [[PubMed](#)]
16. Gu, Y.; Zhang, L.; Yang, J.K.W.; Yeo, S.P.; Qiu, C.W. Color generation via subwavelength plasmonic nanostructures. *Nanoscale* **2015**, *7*, 6409–6419. doi:10.1039/C5NR00578G. [[CrossRef](#)] [[PubMed](#)]
17. Shen, Y.; Rinnerbauer, V.; Wang, I.; Stelmakh, V.; Joannopoulos, J.D.; Soljačić, M. Structural Colors from Fano Resonances. *ACS Photonics* **2015**, *2*, 27–32. doi:10.1021/ph500400w. [[CrossRef](#)]
18. Paniagua-Domínguez, R.; Yu, Y.F.; Miroshnichenko, A.E.; Krivitsky, L.A.; Fu, Y.H.; Valuckas, V.; Gonzaga, L.; Toh, Y.T.; Kay, A.Y.S.; Luk'yanchuk, B.; et al. Generalized Brewster effect in dielectric metasurfaces. *Nat. Commun.* **2016**, *7*, 10362. doi:10.1038/ncomms10362. [[CrossRef](#)] [[PubMed](#)]

19. Zhu, L.; Kapraun, J.; Ferrara, J.; Chang-Hasnain, C.J. Flexible photonic metastructures for tunable coloration. *Optica* **2015**, *2*, 255–258. doi:10.1364/OPTICA.2.000255. [[CrossRef](#)]
20. Gutruf, P.; Zou, C.; Withayachumnankul, W.; Bhaskaran, M.; Sriram, S.; Fumeaux, C. Mechanically Tunable Dielectric Resonator Metasurfaces at Visible Frequencies. *ACS Nano* **2016**, *10*, 133–141. doi:10.1021/acsnano.5b05954. [[CrossRef](#)] [[PubMed](#)]
21. Tseng, M.L.; Yang, J.; Semmlinger, M.; Zhang, C.; Nordlander, P.; Halas, N.J. Two-Dimensional Active Tuning of an Aluminum Plasmonic Array for Full-Spectrum Response. *Nano Lett.* **2017**, *17*, 6034–6039. doi:10.1021/acs.nanolett.7b02350. [[CrossRef](#)] [[PubMed](#)]
22. Duan, X.; Kamin, S.; Liu, N. Dynamic plasmonic colour display. *Nat. Commun.* **2017**, *8*, 14606. doi:10.1038/ncomms14606. [[CrossRef](#)] [[PubMed](#)]
23. Xu, T.; Walter, E.C.; Agrawal, A.; Bohn, C.; Velmurugan, J.; Zhu, W.; Lezec, H.; Talin, A. High-contrast and fast electrochromic switching enabled by plasmonics. *Nat. Commun.* **2016**, *7*, 10479. doi:10.1038/ncomms10479. [[CrossRef](#)] [[PubMed](#)]
24. Chen, Y.; Duan, X.; Matuschek, M.; Zhou, Y.; Neubrech, F.; Duan, H.; Liu, N. Dynamic Color Displays Using Stepwise Cavity Resonators. *Nano Lett.* **2017**, *17*, 5555–5560. doi:10.1021/acs.nanolett.7b02336. [[CrossRef](#)] [[PubMed](#)]
25. Arsenaault, A.C.; Puzzo, D.P.; Manners, I.; Ozin, G.A. Photonic-crystal full-colour displays. *Nat. Photonics* **2007**, *1*, 468. doi:10.1038/nphoton.2007.140. [[CrossRef](#)]
26. Schlich, F.F.; Zalden, P.; Lindenberg, A.M.; Spolenak, R. Color Switching with Enhanced Optical Contrast in Ultrathin Phase-Change Materials and Semiconductors Induced by Femtosecond Laser Pulses. *ACS Photonics* **2015**, *2*, 178–182. doi:10.1021/ph500402r. [[CrossRef](#)]
27. Carlos, R.; Peiman, H.; Taylor, R.A.; Harish, B. Color Depth Modulation and Resolution in Phase-Change Material Nanodisplays. *Adv. Mater.* **2016**, *28*, 4720–4726. doi:10.1002/adma.201506238. [[CrossRef](#)]
28. Raeis-Hosseini, N.; Rho, J. Metasurfaces based on phase-change material as a reconfigurable platform for multifunctional devices. *Materials* **2017**, *10*, 1046. doi:10.3390/ma10091046. [[CrossRef](#)] [[PubMed](#)]
29. Xu, T.; Walter, E.C.; Agrawal, A.; Bohn, C.; Velmurugan, J.; Zhu, W.; Lezec, H.J.; Talin, A.A. High-contrast and fast electrochromic switching enabled by plasmonics. *Nat. Commun.* **2016**, *7*, 10479. doi:10.1038/ncomms10479. [[CrossRef](#)] [[PubMed](#)]
30. Yun, H.; Lee, S.Y.; Hong, K.; Yeom, J.; Lee, B. Plasmonic cavity-apertures as dynamic pixels for the simultaneous control of colour and intensity. *Nat. Commun.* **2015**, *6*, 7133. doi:10.1038/ncomms8133. [[CrossRef](#)] [[PubMed](#)]
31. Yang, B.; Liu, W.; Li, Z.; Cheng, S.; Chen, S.; Tian, J. Polarization-Sensitive Structural Colors with Hue-and-Saturation Tuning Based on All-Dielectric Nanopixels. *Adv. Opt. Mater.* **2018**, *6*, 1701009. doi:10.1002/adom.201701009. [[CrossRef](#)]
32. Goh, X.M.; Zheng, Y.; Tan, S.J.; Zhang, L.; Kumar, K.; Qiu, C.W.; Yang, J.K.W. Three-dimensional plasmonic stereoscopic prints in full colour. *Nat. Commun.* **2014**, *5*, 5361. doi:10.1038/ncomms6361. [[CrossRef](#)] [[PubMed](#)]
33. Ellenbogen, T.; Seo, K.; Crozier, K.B. Chromatic Plasmonic Polarizers for Active Visible Color Filtering and Polarimetry. *Nano Lett.* **2012**, *12*, 1026–1031. doi:10.1021/nl204257g. [[CrossRef](#)] [[PubMed](#)]
34. Li, Z.; Clark, A.W.; Cooper, J.M. Dual Color Plasmonic Pixels Create a Polarization Controlled Nano Color Palette. *ACS Nano* **2016**, *10*, 492–498. doi:10.1021/acsnano.5b05411. [[CrossRef](#)] [[PubMed](#)]
35. Esmaeil, H.; Sperling, J.R.; Neale, S.L.; Clark, A.W. Plasmonic Color Filters as Dual-State Nanopixels for High-Density Microimage Encoding. *Adv. Funct. Mater.* **2017**, *27*, 1701866. doi:10.1002/adfm.201701866. [[CrossRef](#)]
36. Zang, X.; Dong, F.; Yue, F.; Zhang, C.; Xu, L.; Song, Z.; Chen, M.; Chen, P.Y.; Buller, G.S.; Zhu, Y.; et al. Polarization Encoded Color Image Embedded in a Dielectric Metasurface. *Adv. Mater.* **2018**, *30*, 1707499. [[CrossRef](#)] [[PubMed](#)]
37. Nagasaki, Y.; Suzuki, M.; Takahara, J. All-Dielectric Dual-Color Pixel with Subwavelength Resolution. *Nano Lett.* **2017**, *17*, 7500–7506. doi:10.1021/acs.nanolett.7b03421. [[CrossRef](#)] [[PubMed](#)]
38. Duempelmann, L.; Luu-Dinh, A.; Gallinet, B.; Novotny, L. Four-Fold Color Filter Based on Plasmonic Phase Retarder. *ACS Photonics* **2016**, *3*, 190–196. doi:10.1021/acsphotonics.5b00604. [[CrossRef](#)]

39. Babinet, J. Sur les couleurs des réseaux. *Ann. Chim. Phys.* **1827**, *40*, 166–177.
40. Born, M.; Wolf, E. *Principles of Optics: Electromagnetic Theory of Propagation, Interference and Diffraction of Light*; Cambridge University Press: Cambridge, UK, 1999.
41. Ebbesen, T.W.; Lezec, H.J.; Ghaemi, H.F.; Thio, T.; Wolff, P.A. Extraordinary optical transmission through sub-wavelength hole arrays. *Nature* **1998**, *391*, 667. [[CrossRef](#)]



© 2018 by the authors. Licensee MDPI, Basel, Switzerland. This article is an open access article distributed under the terms and conditions of the Creative Commons Attribution (CC BY) license (<http://creativecommons.org/licenses/by/4.0/>).